L-Band Wide Area Surveillance Radar Design Alternatives

Mark E Davis, Braham Himed
Air Force Research Laboratory
Email: Mark.Davis@rl.af.mil , Braham.Himed@rl.af.mil

SUMMARY Wide area surveillance systems are becoming more important for border and homeland security, earth resources monitoring and mitigation of natural disasters such as floods and seismic activity. As the frequency spectrum is being utilized for communications and business networking, the available bandwidth for these important efforts is more difficult. Historically, airborne surveillance radars have been fielded at either UHF or S-Band for airborne vehicle detection, and at X-Band for surface vehicle imaging and moving target detection. This paper will examine the impact of new technologies on the design of L-Band surveillance radars that employ solid state active arrays, multiple phase center apertures and adaptive processing to enable fixed and moving target detection from air and space platforms. The operational advantages of the use of small apertures on business jets, medium apertures on high altitude platforms and very large apertures in space will be contrasted.

I. CONCEPT OF OPERATIONS

A wide area surveillance system is constructed to provide visibility over as wide an area as possible, with revisit times commensurate with the mobility and characteristics of the signatures of interest. These signatures vary from fast airborne vehicles to very slow or stationary structures hidden by trees. The major drivers on area coverage are the altitude of the radar platform and the field of view of the radar sensor. Figure 1 depicts the ground range of coverage for three platforms to be investigated in this paper: business jet, high altitude unmanned air vehicle and low earth orbit satellite.

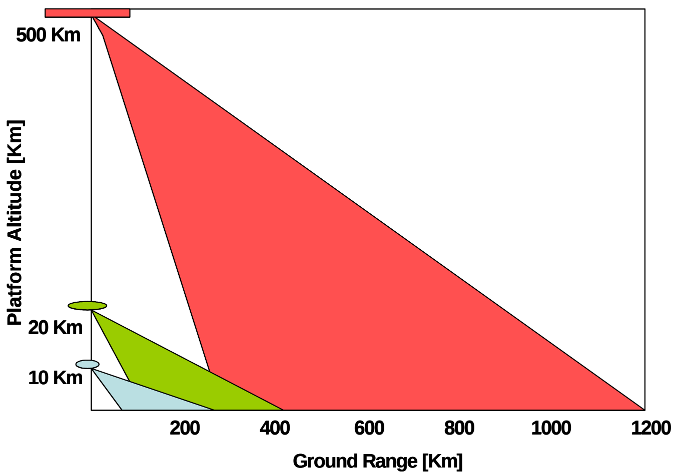

Figure 1 Notional Ground Coverage for 3 Surveillance Radar Platforms

The problem becomes one of defining the following factors in radar system design: [1,2]

- Size of area of interest
- Revisit rate to cover the search volume.
- Multiple mode scheduling --- what other modes need to be scheduled that will affect the area coverage rate.
- Obscuration of targets due to terrain blockage, foliage or other interference effects
- Minimum detectable velocity, or maximum target velocity for waveform design

Table 1 summarizes the first order allocation of these factors to the three platforms, and being used in this tradeoff study. Notice that three “point designs” are being summarized. However, it is anticipated that the eventual system will have significantly more variability in waveforms to meet the demands over the operational conditions of the platforms.

Table 1 Concept of Operations for Wide Area Surveillance Study

Concept of Operations	Business Jet	High Altit. UAV	Low Earth Orbit SBR
Altitude [km]	10	20	500
Velocity [km/sec]	0.25	0.18	7.1
Area of Interest	200 by 200	400 by 400	600 by 600
Revisit Rate [sec]	10 sec	10 , 60 sec	10, 60 sec
Modes	AMTI	AMTI, GMTI	AMTI, GMTI, FOPEN
MDV [m/s]	n/a	5	10
Maximum velocity [m/s]	600	600	600
Antenna Size	4 m x 1 m	8m x 1 m	50m x 2 m
Peak Power	5 kw	5 kw	25 kw
Nel (az by el)	32 by 6	64 by 6	384 by 12
J	32 by 1	32 by 1	32 by 1
Polarization	HH, HV	HH, HV	HH, VV, HV
PRF	1000	300	10000
Duty Factor	0.032	0.038	0.08
Pulse Width [μsec]	32	128	8

Report Documentation Page

Form Approved
OMB No. 0704-0188

Public reporting burden for the collection of information is estimated to average 1 hour per response, including the time for reviewing instructions, searching existing data sources, gathering and maintaining the data needed, and completing and reviewing the collection of information. Send comments regarding this burden estimate or any other aspect of this collection of information, including suggestions for reducing this burden, to Washington Headquarters Services, Directorate for Information Operations and Reports, 1215 Jefferson Davis Highway, Suite 1204, Arlington VA 22202-4302. Respondents should be aware that notwithstanding any other provision of law, no person shall be subject to a penalty for failing to comply with a collection of information if it does not display a currently valid OMB control number.

1. REPORT DATE	2. REPORT TYPE	3. DATES COVERED
14 APR 2005	**N/A**	**-**

4. TITLE AND SUBTITLE
L-Band Wide Area Surveillance Radar Design Alternatives

5a. CONTRACT NUMBER

5b. GRANT NUMBER

5c. PROGRAM ELEMENT NUMBER

6. AUTHOR(S)

5d. PROJECT NUMBER

5e. TASK NUMBER

5f. WORK UNIT NUMBER

7. PERFORMING ORGANIZATION NAME(S) AND ADDRESS(ES)
Air Force Research Laboratory

8. PERFORMING ORGANIZATION REPORT NUMBER

9. SPONSORING/MONITORING AGENCY NAME(S) AND ADDRESS(ES)

10. SPONSOR/MONITOR'S ACRONYM(S)

11. SPONSOR/MONITOR'S REPORT NUMBER(S)

12. DISTRIBUTION/AVAILABILITY STATEMENT
Approved for public release, distribution unlimited

13. SUPPLEMENTARY NOTES
See also ADM001798, Proceedings of the International Conference on Radar (RADAR 2003) Held in Adelaide, Australia on 3-5 September 2003., The original document contains color images.

14. ABSTRACT

15. SUBJECT TERMS

16. SECURITY CLASSIFICATION OF:			17. LIMITATION OF ABSTRACT	18. NUMBER OF PAGES	19a. NAME OF RESPONSIBLE PERSON
a. REPORT	b. ABSTRACT	c. THIS PAGE			
unclassified	**unclassified**	**unclassified**	**UU**	**6**	

Standard Form 298 (Rev. 8-98)
Prescribed by ANSI Std Z39-18

II. SURVEILLANCE RADAR CLUTTER SPECTRUM

The performance of a surveillance radar against ground and airborne targets is determined by the size of an antenna that can be installed, the platform altitude and vehicle speed. The clutter Doppler spectrum is one of the most significant factors affecting target detection. The Doppler on the surface of the Earth as a function of geometry from the platform is given by: [3]

$$f_d = \frac{2v}{\lambda} \cos\theta \sin\phi \, . \qquad (1)$$

For a business or small commercial jet, with a velocity of 250 meters per second, the antenna will be limited to approximately 4 meters in length, Figure 2 depicts the ground clutter Doppler around the platform for a waveform at 1000 Hz, suitable for detecting airborne targets. Superimposed on the Figure are the iso-Range circles, and the iso-Doppler contours. The transmitter mainbeam footprint is also depicted as the ellipse centered at 250 Km range. The waveform selection must consider this clutter return into both the mainbeam and sidelobes of the antenna, along with the fold-over of both range and Doppler ambiguities within the range-Doppler spectrum.

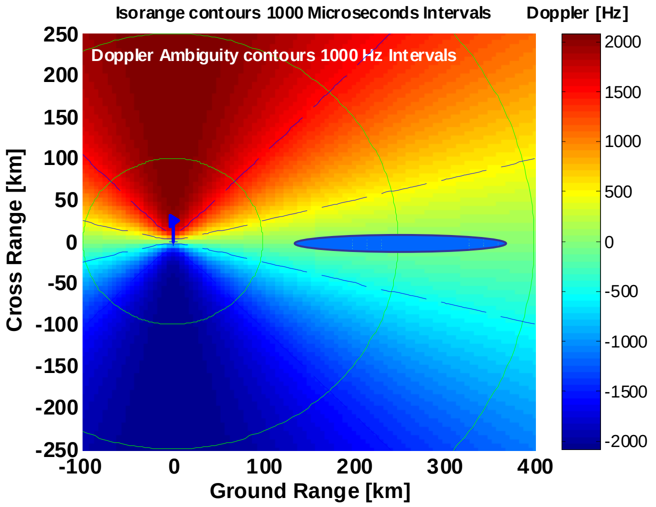

Figure 2 Business Jet Case – 1000 Hz PRF

For GMTI, a range unambiguous PRF is recommended to limit the impact of range ambiguities on adaptive processing. Figure 3 shows the ground clutter spectrum within the field of regard of the radar, from a 300 Hz PRF, for a high altitude UAV. With this LPRF, it is seen that there is only one unambiguous range, centered at a potential target range of 250 Km. However there are several Doppler ambiguities as depicted by the blue contours. These Doppler ambiguities will be important in determining the total unambiguous target Doppler that can be detected.

The space based radar case was chosen for a wide target velocity detection performance, employing a high PRF of 10,000 Hz. is shown in Figure 4. In this case there is significant range ambiguity within the transmitter footprint. This is the result of choosing a PRF sufficient to give wide Doppler visibility for all classes of airborne targets.

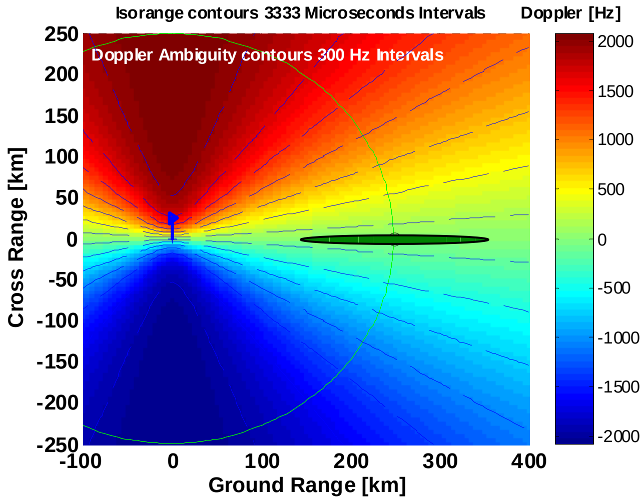

Figure 3 High Altitude UAV Case – 300 Hz PRF

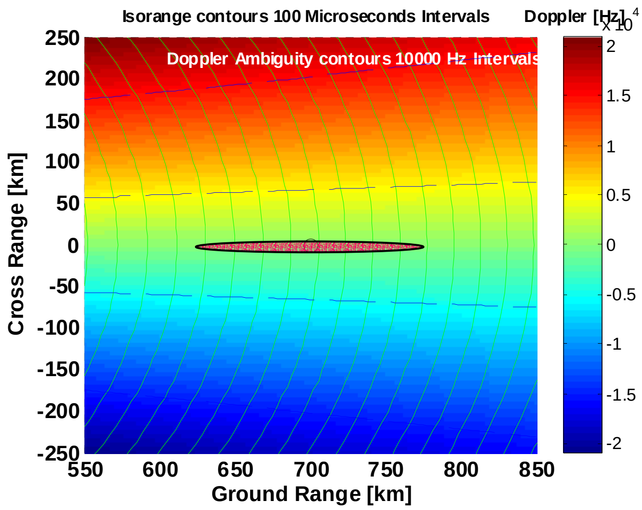

Figure 4 SBR Case – 10,000 Hz PRF

The detection of targets is affected by the width of the mainbeam at the range of interest, the Doppler clutter spread across the mainbeam, clutter signal processing (Doppler and STAP) and the effects of sidelobe energy within the Doppler spectrum that competes with the target.

III. ANTENNA & WAVEFORM IMPACT ON STAP

Space Time Adaptive Processing (STAP) is normally required to remove mainbeam clutter and other interference

that limits the usable Doppler space in the waveform. By sampling the wavefront at several positions separated by d, the spatial and temporal (Doppler) variation of the clutter can be efficiently cancelled providing efficient detection of slow targets. The spatial sampling is represented by spatial frequency parameter:

$$\vartheta_c = \frac{d}{\lambda}\cos\theta\sin\phi \quad \cdot \qquad (2)$$

Normally, the spatial samples are dipole-like and spaced under a half wavelength. In this manner, there are no grating lobes or spatial ambiguities. The clutter Doppler has an identical angular performance (note common terms in (1) and (2)) and the clutter maps into the normalized Doppler vesus sine (ϕ) space as straight line with slope β:

$$\beta = \frac{2vT_r}{d} \;; \qquad (3)$$

where T_r is the pulse repetition interval, and v is the platform velocity.

In the cases studied, only Case 1 is a dipole. It is often impractical to place an analog to digital converter behind each element. As a result, the analysis will consider three antenna subarry configuration cases as shown in Figure 5.

- Case 1 Column subarrays of 1 by 6 elements separated by 0.56 λ
- Case 2 Column subarray of 2 by 6 elements, separated by 1.12 λ
- Case 3 Column subarray of 12 by 12 elements separated by 6.72 λ

Although each subarray is phased to point to the "target", from a spatial sample basis, the clutter will be weighted by the patterns shown in Figure 5, and have grating lobes based on the spacing between the subarrays.

Using the radar parameters outlined in Table 1, the power spectral density of the waveform is calculated for the three cases and shown in Figure 6 to Figure 8.

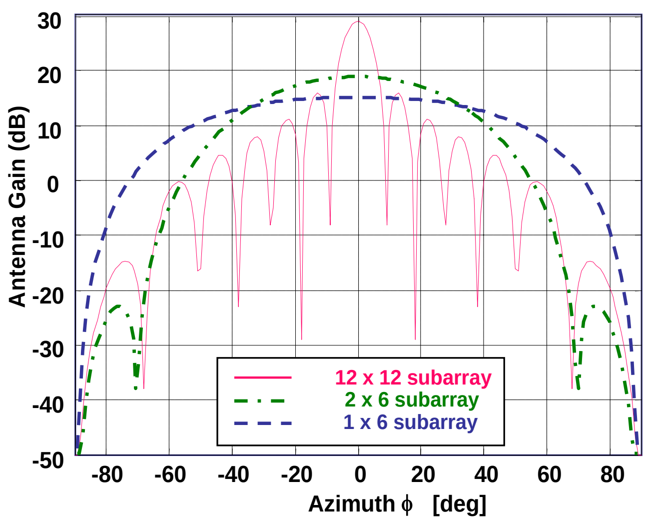

Figure 5 Subarray element pattern for STAP processing

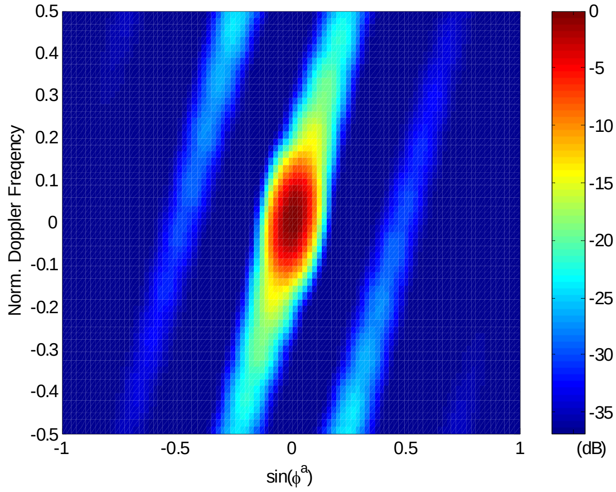

Figure 6 Normalized Doppler vs Sin(ϕ) for Case 1 PRF=1000 Hz, 0.56 λ azimuth spacing

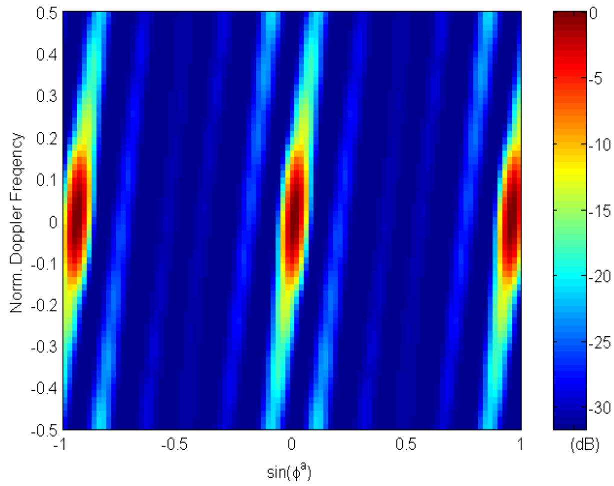

Figure 7 Normalized Doppler vs Sin(ϕ) for Case 2 PRF=300 Hz, 1.12 λ azimuth spacing

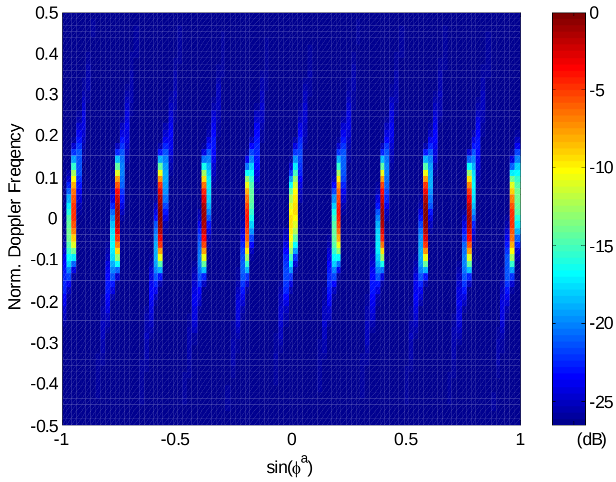

Figure 8 Normalized Doppler vs Sin(ϕ) for Case 3 PRF=10,000 Hz, 6.72 λ azimuth spacing

The clutter spectrum can be examined for principal components by forming an ideal covariance matrix and solving for the eigen values. The rank order of the eigen values is representative of the number of degrees of freedom required to adaptively cancel the interference (clutter). Figure 9 shows the rank order of the eigen values for the three cases presented.

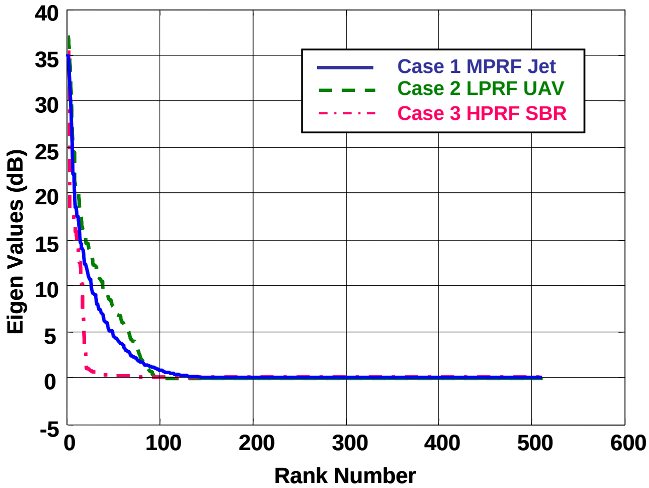

Figure 9 Rank Order of Eigen Values for 3 Lband Cases

From Brennan's Rule, the expected number of degrees of freedom to cancel the clutter interference is related to the number of temporal degrees of freedom (N) and the spatial degrees of freedom (J), and the clutter ridge slope (b) by: [3]

$$r_C \approx \left[N + (J-1)\beta\right] . \tag{4}$$

Table 2 summarizes the parameters for the three cases along with the rank of the clutter. There is excellent agreement between the Brennan rule and the eigenvalue analysis, despite the effects of spatial ambiguity shown in the periodograms.

Table 2 Comparison of Radar Waveform and Antenna DOF and Clutter Rank using Brennan's Rule

	Case 1 Jet	Case 2 UAV	Case 3 SBR
Spatial DOF -- J	32	32	32
Temporal DOF -- N	16	16	16
Spatial Sample Distance – d/λ	0.56	1.12	6.72
Clutter slope -- β	4.0	4.8	0.9
Clutter Rank -- r_C	92	103	44

IV. ADAPTIVE PROCESSING

From the discussion in the previous section, it is apparent that ground clutter will occupy a significant portion of the unambiguous Doppler space. In order to detect either slow moving ground targets, or airborne targets over a significant range of velocities, it will be necessary to utilize adaptive processing to cancel the mainbeam clutter and maintain detection on the target. This section will provide a first order assessment of the adaptive processing limits given the antenna and waveform details presented above.

Consider a radar receiver system with J spatial channels and N pulses in a coherent processing interval (CPI). In concatenated form, the received signal can be written as a (JNx1) vector given by

$$\boldsymbol{x} = \boldsymbol{t} + \boldsymbol{i} + \boldsymbol{c} + \boldsymbol{n}, \tag{5}$$

where **t**, **i**, **c**, and **n** are the target, jamming, clutter, and additive white noise vectors, respectively. It has been shown [4] that given an observation data vector **x**, the STAP system is an adaptive filter with a JN×1 weight vector ***w***. The optimum weight vector that produces the maximum output signal-to-interference (clutter and jamming) plus noise ratio (SINR) is given by

$$\boldsymbol{w} = \alpha \boldsymbol{R}_{\mathrm{x}}^{-1} \boldsymbol{t} , \tag{6}$$

where α is an arbitrary constant, and $\boldsymbol{R}_x$ is the interference and noise covariance matrix. The maximum output SINR is then given by

$$\boldsymbol{SINR}_{max} = \boldsymbol{t}^H \boldsymbol{R}_x^{-1} \boldsymbol{t} . \tag{7}$$

where the superscript "*H*" denotes the Hermitian transpose.

In practice, both $\boldsymbol{R}_x$ and $\boldsymbol{t}$ in Equation (6) are unknown 'a priori'. Therefore, the maximum SINR of Equation (7) is never achieved. A 'search' steering vector (often measured), ***s***, is used to replace the target signal vector and the covariance matrix is replaced by its estimate $\hat{\boldsymbol{R}}_x$. The weight vector can be estimated using

$$\hat{\boldsymbol{w}} = \alpha \hat{\boldsymbol{R}}_{\mathrm{x}}^{-1} \boldsymbol{s} . \tag{8}$$

The conditioned output SINR using the estimated covariance matrix case has been shown to be

$$\mathrm{SINR} = \frac{\left| \boldsymbol{s}^{\mathrm{H}} \hat{\boldsymbol{R}}_{\mathrm{x}}^{-1} \boldsymbol{t} \right|^2}{\boldsymbol{s}^{\mathrm{H}} \hat{\boldsymbol{R}}_{\mathrm{x}}^{-1} \boldsymbol{R}_{\mathrm{x}} \hat{\boldsymbol{R}}_{\mathrm{x}}^{-1} \boldsymbol{s}} . \tag{9}$$

To conduct our analysis, the true "known' covariance matrix ***R*** and time series data have been generated for each case. For the first two cases, K = 1201 range cells have been generated symmetrically around the test cell (primary cell) assumed to be at range cell 601. This number K is more than twice the number of degrees of freedom needed to estimate the sample covariance matrix; i.e.; Brennan' rule is well exceeded in this case.

The analysis was conducted using the matched filter (MF) and its adaptive counterpart, referred to as adaptive matched filter (AMF). To complete our analysis, we also provided the output SINR for several reduced rand/dimension STAP methods. These include the Joint-Domain Localized (JDL) [5] approach, the Factored Time Space (FTS) [6] approach, the Extended Factored Approach (EFA) [7], and the Parametric Adaptive Matched Filter (PAMF) [8]. A comparative analysis was then conducted to assess the performance of the above mentioned STAP approaches.

Figure 10 shows the normalized output SINR as a function of target velocity for the airborne case, where a PRF rate of 1 kHz was assumed. Note from this Figure, that the AMF performs very poorly, although an ideal assumption was made in terms of a homogeneous background. Further analysis of the AMF, not shown here, assuming diagonal loading (often referred to as hard constraint) shows that the AMF still fails to approach the MF performance. This is in part due to the ambiguous (range and Doppler) nature of the clutter. The same argument could also be made about the JDL, FTS, and EFA approaches. Their inability to properly cancel the clutter is clearly shown in Figure 10. On the hand, the PAMF, with a filter model order of 1 performs relatively better, although there are still significant losses in output SINR. It is our belief that the performance of the PAMF could considerably improved if more pulses are used, since the filter coefficients are estimated using pulse averaging. In this case only 16 pulses have been generated to speed up the data generation process. In the future, we will increase this number to around N = 256 since J = 32 spatial channels are considered and the PAMF works best if N=4J.

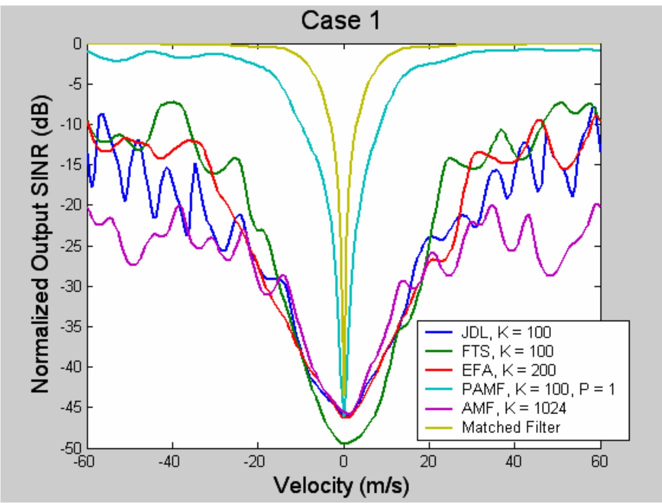

Figure 10 Normalized Output SINR vs. Target Velocity

Figure 11 shows the performance of the above mentioned approaches in the Case 2. From this Figure, we can see again the failure of the AMF to effectively cancel the ground clutter. JDL, FTS, and EFA also perform very poorly. The PAMF, with model order P = 1 performs better, but the minimum discernable velocity (MDV) still suffer considerably. On going research is being carried out to properly cancel the ground clutter.

Figure 12 shows the performance of the proposed approaches for the space-based Case 3. In this case, because of system parameters, we only generated K = 211 range cells, a number way below the required 2JN criterion. To properly use the AMF, a hard constraint was used, whereby 10 dB diagonal loading was used. Note from this Figure that all proposed approaches fail to cancel the ground clutter, since the system is Doppler ambiguous and highly range ambiguous. This is a known fact in the STAP community and research is being conducted to alleviate this problem.

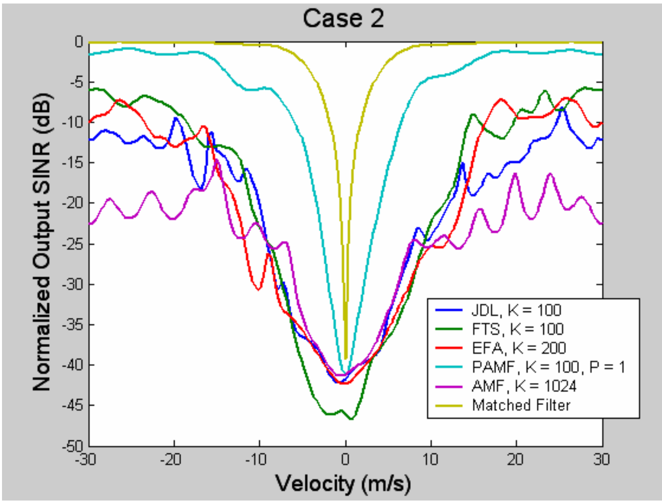

Figure 11 Normalized Output SINR vs. Target Velocity

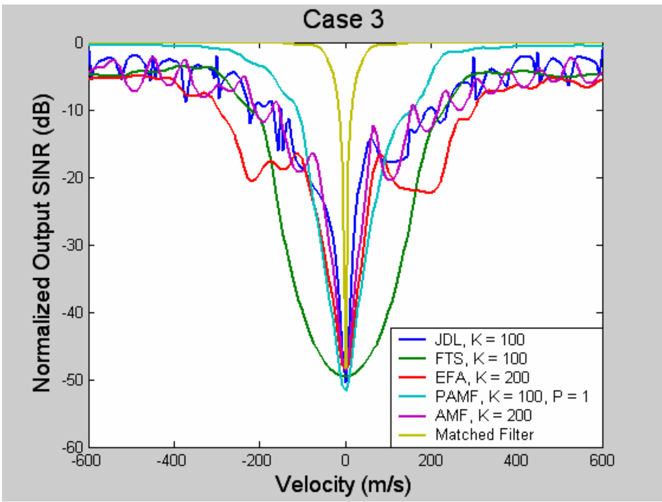

Figure 12 Normalized Output SINR vs. Target Velocity

V. FUTURE RESEARCH REQUIREMENTS

The ability to detect slowly moving targets in clutter with an antenna that is small compared to the unambiguous Doppler space requires special consideration. The obvious first order solution is to employ Space Time Adaptive Processing with a multiple channel antenna to isolate the target Doppler from the mainbeam Doppler spread. This has been an area of intense research over the past 10 years. The system architectures presented in this work assume STAP as a first order system requirement. However, the assumptions for effective STAP operation are many: independent identically distributed samples to estimater the covariance matrix; well matched channels in the spatial and spectral regimes, and stationarity of the target and clutter during the adaptive processing periods. This approach requires an accurate simulation and measurements of airborne or spaceborne radar in a relevant environment.

It is clear from the previous section that a reduction of sidelobe clutter returns is required. The current cases considered uniform transmitter illumination. What is needed is further analysis of amplitude taper on transmit, considered to be beyond current active array capabilities. This will serve as motivation for further active ESA development.

A second system application of L-Band surveillance from an airborne or spaceborne platform is the ability to see targets in foliage. Davis [9] has outlined many of the system requirements for efficient foliage penetration SAR including a loss model versus frequency and grazing angle. There is evidence that L-Band provides some degree of detection of targets under sparse foliage, and may enable the detection of moving targets if the loss and endoclutter interference is not excessive. For a surveillance radar designed for area coverage rate against aircraft size targets, the average power will be sufficient to provide detection of ground targets under this foliage coverage. The challenge is presented by requirement for polarization diversity for fixed targets, and effects of internal clutter motion on detection of moving targets. The waveforms need to be revisited to enable two – polarization transmit within radar duty factor limitation.

Finally, for a space based surveillance radar the ionosphere presents a unique set of system requirements. Tulley [10] has recently examined the design for a UHF radar from space. The impact of ionospheric scintillation on the allowed coherent integration times will affect the efficiency of detecting targets and maintaining required area coverage rates. The current work synthesized the detection of targets with limitations on CPI, frequency agility and polarization agility to maintain a detection probability, and the effects of beamsize on total surveillance volume. Future analysis is needed to evaluate the effects of ionospheric dispersion and scintillation on the ability to adaptively remove the ground clutter.

VI. SUMMARY

Several new surveillance radar systems are under consideration for regional and global detection of both ground and airborne moving targets. L-Band is one of the frequency bands that have been allocated world wide for radar operations. This paper outlines the primary radar system design considerations for a multimode radar that can accomplish synthetic aperture radar detection of fixed targets, low PRF operation for detection of slow moving targets, and high PRF operation for airborne radars. Significant design challenges for applications of these three modes are being solved with recent advances in waveform synthesis and space time adaptive processing.

REFERENCES

[1]. Davis, ME "Technology Challenges for Space Based MTI Radars" Proceedings IEEE 2000 International Radar Conference, Washington DC, May 2000, p.18

[2]. Rosen, PA, and ME Davis, "A Joint Space-Borne Radar Technology Demonstration Mission for NASA and the Air Force", Proceedings IEEE 2003 Aerospace Conference, Big Sky MT, March 2003

[3]. Ward J "Space Time Adaptive Processing for Airborne Radar" MIT Lincoln Laboratory Technical Report ESC-TR-94-109, 1994

[4]. L. E. Brennan et al., "Theory of adaptive radar," *IEEE Trans. AES*, AES-9, pp. 237-251, March 1973.

[5]. A. D. Jaffer et al., "Adaptive space-time processing techniques for airborne radars," RL-TR-91-162, 1991.

[6]. R.C. DiPietro, "Extended factored space-time processing for airborne radar," *Proc. 26-th ASILOMAR Conf.*, Pacific Grove, CA, pp. 425-430, October 1992.

[7]. H. Wang et al., "On adaptive spatio-temporal processing for airborne surveillance radar systems," *IEEE Trans. AES*, AES-30, pp. 660-670, July 1994.

[8]. M. Rangaswamy, J. H. Michels, "A parametric multichannel detection algorithm for correlated non-Gaussian random processes," 1997 IEEE National Radar Conf., pp. 349-352, 13-15 May, 1997.

[9]. Davis ME, Tomlinson PG, Maloney RP, "Technical Challenges in Ultra Wideband Radar Development for Terrain Mapping", Proceedings IEEE 1999 Radarcon, Boston MA, May 1999

[10]. Tuley, MT, TC Miller, RJ Sullivan " Ionospheric Scintillation effect on a Space Based Foliage Penetration Ground Moving Target Indication Radar" Institute for Defense Analyses Document D-2579, Alexandria VA. Jan 2003